Centrifuge modeling technique for axial compressive loading on helical piles in sand

Naveel Islam, Lijun Deng, Rick Chalaturnyk
Department of Civil & Environmental Engineering-University of Alberta, Edmonton, Alberta, Canada
& Luke Penner
Reaction Piling Inc., Nisku, Alberta, Canada

GeoCalgary 2022 October 2-5
Reflection on Resources

ABSTRACT
Model helix piles in previous research based on geotechnical centrifuge modeling were insufficiently instrumented and characterized. As a result, there is a knowledge gap on the appropriate experimental technique that can provide accurate information on the internal load transfer within the helices and the nature of pile failure mode, particularly in the sand. The article provides an overview of the pile instrumentation and centrifuge modeling technique and axial compressive load carrying capacity on five model aluminum piles in a model box filled with sand. For instrumentation, two groove trenches were engraved onto the sides of the metal shaft to place axial strain gauges at definite locations over the length of the pile. Appropriate calibrations were made to ascertain the accuracy of the placed gauges over some fixed loads. An appropriate sand pluviation technique was adopted, and correlation charts were developed for a prefabricated portable traveling pluviator to obtain the uniformity of sand deposition on the model box for a desired relative density. A dual-axis electrical actuator was affixed on top of the soil container to impose the axial compressive load on the installed model piles in the sand bed. From an inflight centrifuge test at a 20 g scale unit, the axial load vs. normalized axial displacement responses of the model piles up to a depth of 20% of the shaft or helix diameter is ascertained from the axial strain gauges located within the pile. It was observed that, the pile with helix carried a larger load compared to a smooth pile. With the addition of a second helix and an increase in inter helix spacing, the load-carrying capacity increases significantly, depicting the nature of a Cylindrical Shear Mode (CSM). The measured ultimate capacity was comparable to the theoretical ultimate capacity from the literature.

RÉSUMÉ
Les modèles de pieux hélicoïdaux dans les recherches précédentes basées sur la modélisation géotechnique par centrifugation étaient insuffisamment instrumentés et caractérisés. En conséquence, il existe un manque de connaissances sur la technique expérimentale appropriée qui peut fournir des informations précises sur le transfert de charge interne dans les hélices et la nature du mode de rupture du pieu, en particulier dans le sable. L'article donne un aperçu de l'instrumentation des pieux et de la technique de modélisation par centrifugation et de la capacité de charge de compression axiale sur cinq pieux modèles en aluminium dans une boîte modèle remplie de sable. Pour l'instrumentation, deux tranchées à rainures ont été gravées sur les côtés de l'arbre métallique pour placer des jauges de contrainte axiale à des emplacements définis sur la longueur du pieu. Des étalonnages appropriés ont été effectués pour vérifier la précision des jauges placées sur certaines charges fixes. Une technique appropriée de pluie de sable a été adoptée et des tableaux de corrélation ont été développés pour un pluviateur portable préfabriqué afin d'obtenir l'uniformité du dépôt de sable sur la boîte modèle pour une densité relative souhaitée. Un actionneur électrique à double axe a été fixé au-dessus du conteneur de sol pour imposer la charge de compression axiale sur les pieux modèles installés dans le lit de sable. À partir d'un essai de centrifugation en vol à une unité d'échelle de 20 g, la charge axiale par rapport aux réponses de déplacement axial normalisé des pieux modèles jusqu'à une profondeur de 20 % du diamètre de l'arbre ou de l'hélice est déterminée à partir des jauges de contrainte axiales situées dans le pieu. Il a été observé que le pieu avec hélice portait une charge plus importante par rapport à un pieu lisse. Avec l'ajout d'une deuxième hélice et une augmentation de l'espacement entre les hélices, la capacité de charge augmente considérablement, illustrant la nature d'un mode de cisaillement cylindrique (CSM). La capacité ultime mesurée était comparable à la capacité ultime théorique de la littérature.

1 INTRODUCTION

Helical piles, also known as screw piles, helical piers, or helical anchors, are innovative deep foundation types that carry compressive, tensile, lateral, and cyclic loads. It is relatively quick in installation with minimal environmental impacts and has wide applications in the construction industry. Unlike a conventional pile with a smooth shaft, metal helix plates are welded onto the shaft to provide additional bearing surfaces. As per industrial need, the number and spacing of the helices are varied from one pile to the other.

A study of the axial behavior of helical piles in sand soil sites is continued research. Several researchers in the past performed full-scale field tests (e.g., Zhang (1999), Sakr (2009), Livneh and El Naggar (2008), Elsherbiny and El Naggar (2013), Tsuha et al. (2013), Nabizadeh and Choobbasti (2016) to ascertain the compressive and tensile capacity of such piles. However, field tests are affected by the prohibitively high cost of testing of piles, particularly when the piles are grouped to support a combination of loads. Some researchers also attempted lab-scale model tests (e.g., Clemence and Pepe (1984), Mitsch and Clemence (1985), Ghaly et al. (1991), Nagata

and Hirata (2005), Arai et al. (2011), Schiavon et al. (2013), Spagnoli et al. (2015)). However, most of these small-scale tests were limited to its outcome because of boundary effects and model size dimension. A viable solution to the limitations of lab-scale models was to adopt the centrifuge modeling technique for helical pile research. Centrifuge modeling of soil-pile interaction can significantly reduce the cost of field testing while still simulating the appropriate mechanism of piles in the field.

Levesque et al. (2003) were the first to perform centrifuge modeling tests on helical piles to verify the analytical uplift resistances for varying densities of sand. Bian et al. (2008) performed centrifuge tests by grouting through central shafts to address issues related to foundation strengthening. Tsuha et al. (2007, 2012) tested deep helix piles to study the tensile performances in varying density sands. Urabe et al. (2015) also studied the effect of pullout resistance on helical piles. Some other researchers also performed centrifuge tests to ascertain the load-carrying capacity but are limited to marine renewable or offshore wind energy applications only (e.g., Al-Baghdadi et al. (2016), Schiavon et al. (2016), Brown et al. (2019)). However, most of the helix pile tests were insufficiently instrumented and characterized. The lack of instrumentations at each pile segment leaves a knowledge gap on the internal load transfer within the piles. Li et al. (2022) pioneered research in centrifuge tests for instrumented helix piles in clay to measure the axial load distribution and installation torques. However, there is a clear need for understanding the axial load carrying capacity for instrumented helix piles in the sand beyond the recommended failure load (In general practice, 5 to 10% of the helix diameter) when the piles are subjected to axial loads, individually or in groups. Moreover, the current widespread use of such piles in the construction industries in Canada demands knowledge on the potential benefits of additional helices with varied inter helix spacing.

The present study aims to provide an overview of the pile instrumentation and centrifuge modeling technique adopted to study helical piles installed in silica sand. Later, the axial compressive load to axial displacement responses of five different helical piles are presented. The 2-m radius Broadbent Centrifuge facility (GeoCERF) at the University of Alberta was used for the test. Commissioned in 2012, the GeoCERF centrifuge became the first and is the only one of its kind in Western Canada. Pioneered in extensive research in assessing shallow caprock failure and consolidation of oil sand tailings, it was advanced for research on soil-helix pile interaction (Islam et al. 2020).

2 CENTRIFUGE TESTING PROGRAM

The present program (NI01a) is a part of a series of tests NI01. In NI01a, five model piles were tested in axial compressions in a model silica sandbox. Fig. 1a shows the test layout plan. The piles were designated as **PXC**, where P stands for pile, X stands for pile number, and C stands for loading type. The smooth pile without helix is denoted as P0C, and helix piles, as P1C to P4C. Fig. 1b shows the vertical profiles of the installed piles at two cross-sections, A-A and B-B, of the model box. The centrifugal acceleration was set at a 20 g scale for the tests. Model scale factors of the analyzed parameter are listed in Table 1.

The five model piles were installed at a 1 g scale and later loaded in compression at a 20 g scale in each test stage. After each test, the model pile was reinstalled from the model sandbox before moving on to the next test pile. The pile-pile spacing in rows was maintained at least four times the helix diameter and along the diagonal, at least

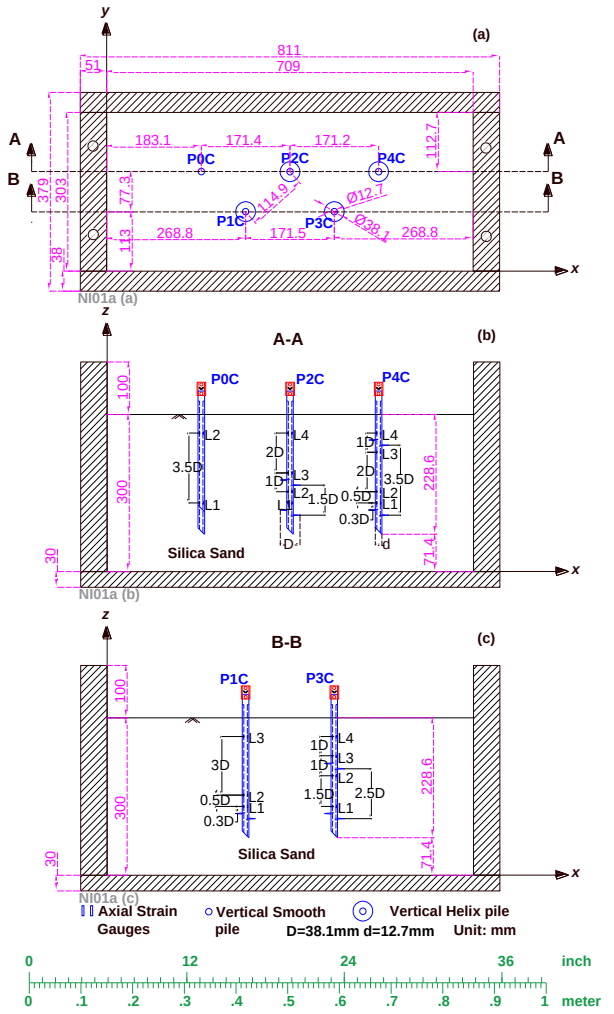

Figure 1. (a) Layout plan of test NI01a; (b) Cross-sectional profile at A-A section; and (b) Cross-sectional profile at B-B section. All dimensions are in model scale.

three times the helix diameter; to minimize the pile installation and test zone interference.

Table 1. Selected scale factors (prototype/model) of centrifuge modeling tests.

Term	Force	Dimension	Stress
Scale Factor	400	20	1

2.1 Soil properties and soil model construction

The silica sand (Sil-3) supplied by Sil Industrial Minerals in Edmonton, Alberta, was used to prepare the sand model box. The geotechnical properties of Sil-3 sand are summarized in Table 2. The particle size distribution (PSD) of Sil-3 sand is shown in Fig. 2. From the PSD, the estimated, d_{50} = 0.29 mm, C_u = 1.5 mm and C_c = 1.08 mm, indicates uniform distribution of grain sizes. As per Schiavon et al. 2016, effective model sand for centrifuge test of helix piles should carry uniformly distributed grain sizes, should not contain a lot of fine sand dust and maintain the ratio of the effective helical radius of the model helix piles (r_h) to the average grain size (d_{50}) of the sand, r_h / d_{50} greater than 58. Hence, for Sil- 3 as model sand, the r_h of the model piles was kept greater than 16.82 mm (discussed in the following section).

Direct shear tests were performed on the model sand at a shear strain rate of 0.76 mm/min. Fig. 3 shows the shear and volume change behavior of the model Sil-3 sand. Tests were conducted for normal loads of 50,100,200 and 400 kPa. The measured constant volume friction angle (ϕ_{CV} = 31.2 deg.) of sand falls within the range of values of shearing resistance of cohesionless soils for sandy silts or silty sands (after AS 4678-2002). Bolton (1986) noted that for most natural sands the ϕ_{CV} ranges between 30 -33 deg. The geometrically measured dilation angle from the slope of volume change to shear strain ranged between 10.2 deg. to 11.2 deg. It is to note that, for normal stresses > 100 kPa, dilation angle for granular soil ranges between 10-20 deg. (Bolton 1979, 1986).

Table 2. Geotechnical properties of model silica sand

Term	Value
Unit density (ρ), Mg/m^3	1.61
Constant Volume Friction angle (ϕ_{cv}), deg.	31.2
Maximum Dry Density (ρ_{max}), Mg/m^3	1.73
Minimum Dry Density (ρ_{min}), Mg/m^3	1.52

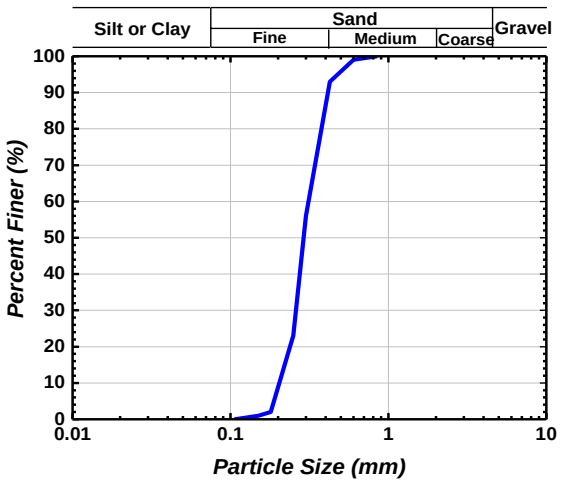

Figure 2. Particle size distribution of model silica sand.

The soil model was constructed in an aluminum container. The container measures internally, 709.2 mm (length), ×300 mm (width) × 400 mm (height) with wall thickness ≥ 30 mm. The model sand deposition was controlled with a portable traveling pluviator (PTP) setup to allow uniform density deposition of sand at each layer in the model box. Fig. 4. shows the various components of the PTP setup for the Sil-3 sand deposition in the model box.

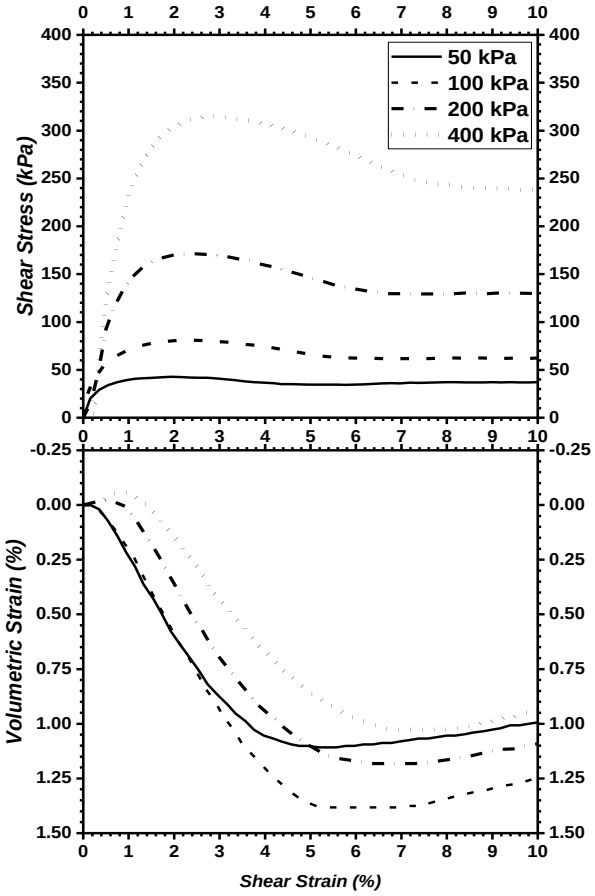

Figure 3. Direct shear test results for the model Sil-3 sand.

Fig. 5. presents the calibration chart developed to ascertain the relationship between the relative density of sand with the height of fall of sand from the PTP to the model box for mesh openings of 5 mm and 10 mm, respectively. The height of fall varied between 110 cm to 150 cm to deposit the sand in a density mold. Later, the relative density of sand for each calibration test was determined. As observed in Fig. 5, the relative density ranged between 72 to 100 % for 10 mm mesh opening and 46 to 86 % for 5 mm mesh opening. For test NI01a, the relative density was fixed at 55%, which corresponds to a height of fall of 114 cm at the PTP. The quality of deposition of sand in the model box was verified using the small container method (see Choi et al. 2010 and Tabaroei et al. 2017) and was not elaborated here for brevity.

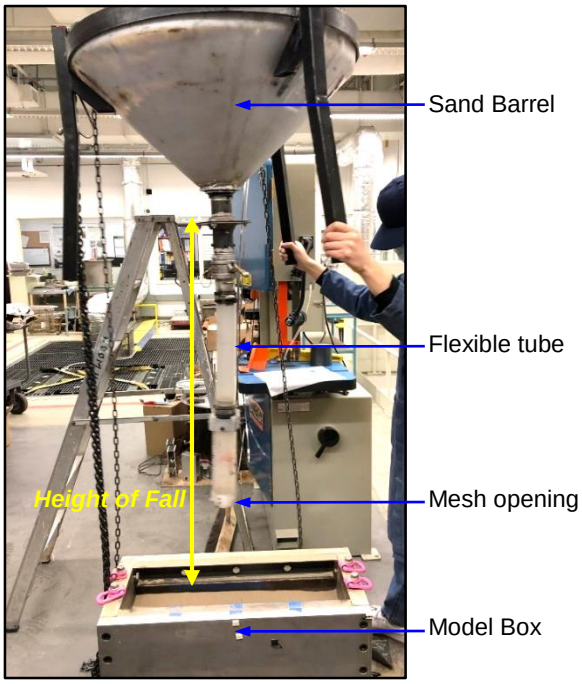

Figure 4. Portable traveling sand pluviator setup.

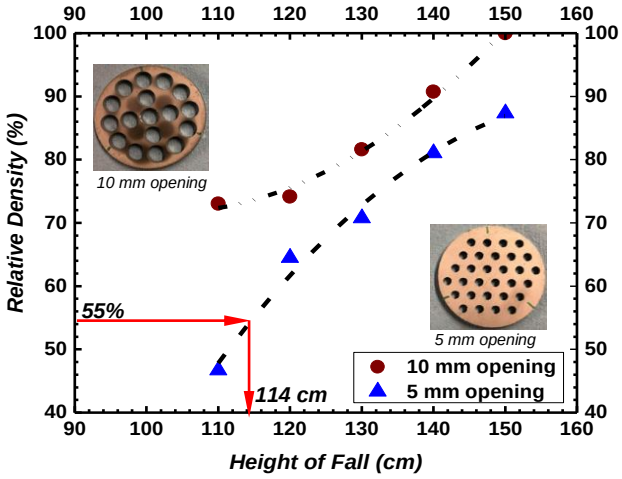

Figure 5. PTP calibration chart for the relationship between the relative density of sand with Height of Fall for two mesh openings.

2.2 Model piles & Instrumentation

Five types of aluminum model piles, i.e., one smooth (P0C), one single-helix (P1C), and three double-helix piles with helix spacing ratio (S_r) of 1.5 (P2C), 2.5 (P3C), and 3.5 (P4C) were fabricated with a better-controlled pitch size of the helices (see Fig. 6). Table 3 lists the summary of test pile geometry in model and prototype scaled units. The prototype shaft diameter, (d) 254 mm, and the helix diameter, (D) 762 mm are common in practice. The pitch of the helices (P), defined as the opening size of the helix, is 12.7 mm in model scale units, equivalent to P = 254 mm in prototype scaled units.

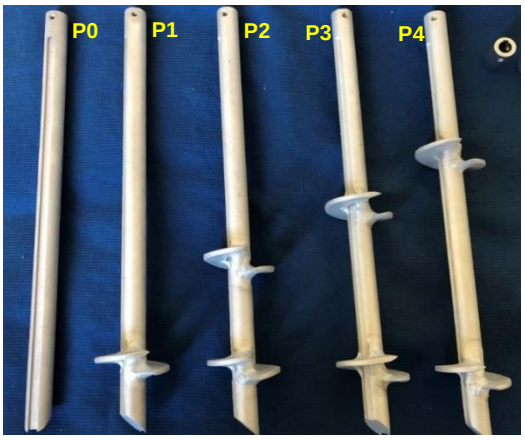

Figure 6. Fabricated Model Piles

Axial strain gauges (SGs) were installed at designated locations along the pile shaft inside the grooved trench (see in Fig. 6 and 7). The SGs are marked from L1 from the tip end to L4 at the top end. The trench protects the SGs from external loading effects and guides the wires. The SGs are meticulously glued inside the trench arrangement and later sealed with protective coatings, Teflon tapes, and epoxy. The surface of the hardened epoxy was smoothed with sanding tools and later polished. To avoid the possibility of the bending effect of the helices, the SGs were placed at a minimum distance of 10 mm away from the helix blades.

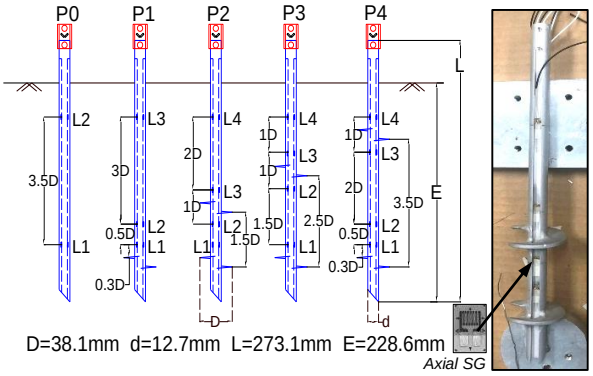

Figure 7. Axial Strain Gauge Instrumentation on Model Piles.

Laboratory calibration tests were conducted on the model piles with installed axial SGs over a sequence of hanged dead loads. Fig 8 (a-b) shows the calibration load arrangement setup for axial and torque strain gauges. The wires running from the axial SGs placed at the trench of the piles are connected to the HBM Data Logger MX1615 B and are read through the computer program CATMAN (see Fig. 8 (a)). The axial SGs were wired into Wheatstone half-bridge circuit. The temperature was maintained constant in the centrifuge chamber room with a variation of ± 0.05 °C; hence a temperature compensation for the axial SGs was considered insignificant for the present case. The tests also confirmed negligible development of bending-induced axial strains in the model piles. Increment weights are placed

from the bottom that develops the requisite axial strain on the piles. The measured strains from the axial SGs were consistent with the theoretical values of strains.

Fig. 8 (b) shows the arrangement setup for torque SG calibration. A set of torque SG is placed on the collar shown. Torque strings are hungover metal support that develops the required torque with incremental loads at the loading ramp at the bottom. The torque SGs are connected with a Wheatstone full-bridge circuit. Similarly, SG wires were run from the SG to the HBM Data logger and read through the computer program, CATMAN.

The applied torque develops a twisting motion within the pile that develops the shear strain, which was comparable to the measured values of shear strains from the data logger. Finally, calibration factors were calculated for each axial SGs in each pile and torque SG at the collar for later use in centrifuge data analyses.

Table 3. Summary of test pile geometry

	Type	No. of helices	Shaft dia. d (mm)	Helix Dia. D (mm)	Pile Length L (mm)	Helix Spacing S (mm)	Lower Helix Embedment E (mm)	$S_r = (S/D)$
Model Scale Unit	P0	0	12.7	38.1	271.8	NA.	150	NA.
	P1	1	12.7	38.1	271.8	NA.	150	NA.
	P2	2	12.7	38.1	271.8	57.2	150	1.5
	P3	2	12.7	38.1	271.8	95.2	150	2.5
	P4	2	12.7	38.1	271.8	133.4	150	3.5
Prototype Scale Unit	P0	0	254	762	5436	N.A.	3000	N.A.
	P1	1	254	762	5436	N.A.	3000	N.A.
	P2	2	254	762	5436	1144	3000	1.5
	P3	2	254	762	5436	1905	3000	2.5
	P4	2	254	762	5436	2668	3000	3.5

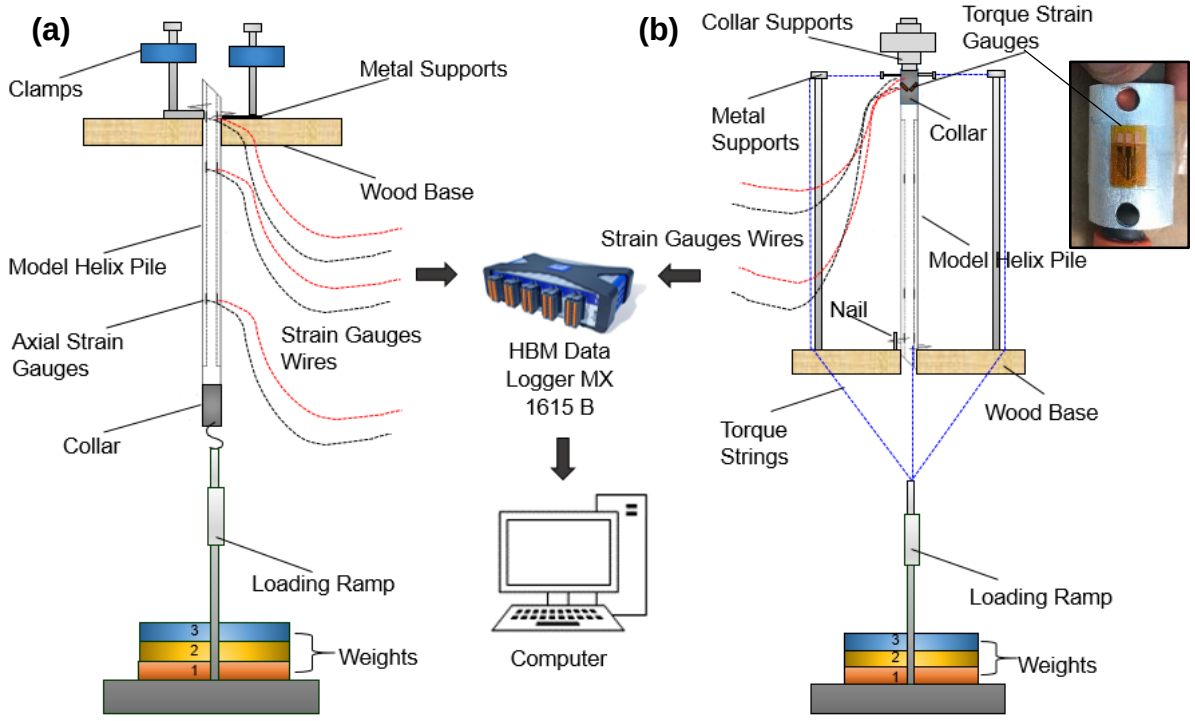

Figure 8. Strain Gauge Calibration Setup: (a) For Axial SGs and (b) Torque SGs.

2.3 Centrifuge Model Box Configuration

Fig. 9(a) presents the model box setup on the centrifuge beam platform with the installation and loading assembly. There are three major parts: the dual-axis electric actuator on the top for vertical movement of piles, the constant rpm gear motor for pile installations mounted to the actuator, and the model soil box with the prepared sand bed. Fig 9(b) shows an installed model pile at a 1 g condition in the sand bed. The piles are installed, maintaining the standard practice of installing the piles at a penetration rate of one pitch of the helix per revolution to keep the soil disturbance

minimal. Thus, the piles were installed at a 23 revolution per min (rpm) rotational rate. Simultaneously, an axial displacement rate of 292.2 mm/ min (= 23 × P/min) was maintained using the electric actuator. Axial SGs are run from the model piles into the data logger affixed on the bottom of the centrifuge platform out of the model box.

In NI01a, the axial compressive loading tests at a 20 g scale were performed by pushing the electric actuator at a constant 0.333 mm/min rate. The constant rate test has also been used in centrifuge tests of helix piles in the literature (e.g., Tsuha et al., 2007, Wang et al., 2013, Li et al., 2022).

3 AXIAL COMPRESSIVE BEHAVIOUR OF PILES

The compressive load vs. normalized displacement responses of the modeled piles are presented in Fig. 10. All the piles were loaded up to a maximum normalized displacement of 20 %.

The load-displacement responses were measured at each of the axial SG stations. For example, L1 indicates the response of SG at the tip end and L4 at the rear end of the pile. The load response for the SG, L4 was the highest, gradually decreasing with depth to SG, L1. All the curves depict the typical axial pile behavior of piles embedded in the sand.

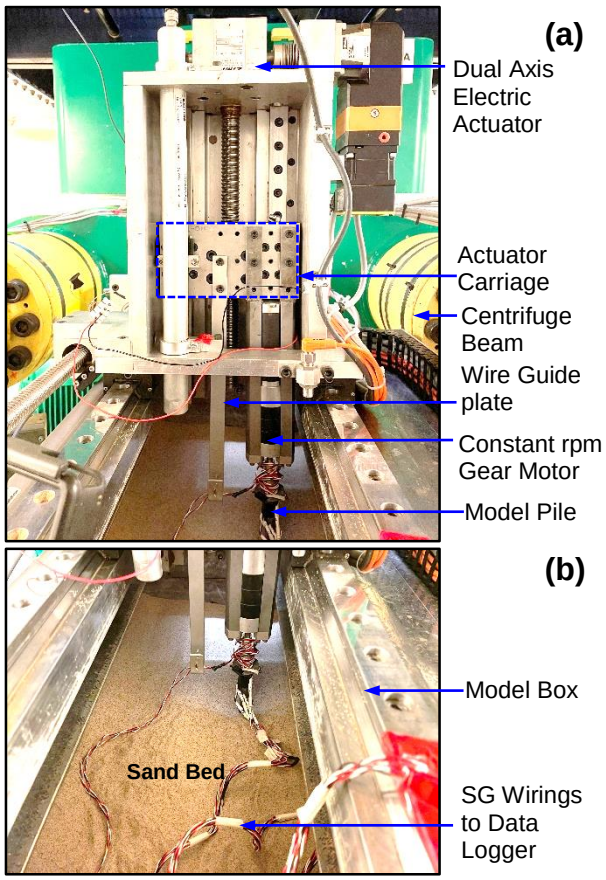

Figure 9. Centrifuge Model Assembly.

For P0C, the smooth pile without helix, the failure load is defined by the stage where the axial movement reached 15% of the shaft diameter (ASTM D1143). For the helix piles (P1C-P4C), the failure load is stated at displacements corresponding to 5% of the helix diameter as commonly practiced in the industry for ultimate capacity predictions in sandy soil (Reese and O'Neill 1988, Sakr 2011, Elsherbiny et al. 2013). There is a gradual increase in the load with increased axial displacement. The load-carrying capacity was significantly higher in piles with helices (P1C to P4C) compared to no helix pile P0C. The second helix piles were added in piles P2C, P3C, and P4C. The measured ultimate capacity (Q_u) increased with inter helix spacing from 1.5 to 2.5 to 3.5.

The theoretical Q_u of the smooth pile (P0C) was estimated using Eq. 1 and that of the helix piles (P1C-P4C) from Eq. 2 following the Canadian Foundation Engineering Manual (CFEM 2006).

For smooth piles

$$Q_u = \pi d E \sigma_v K_s tan\delta + N_t \sigma_v A_s \quad [1]$$

and for helix piles:

$$Q_u = \gamma H_b A_b N_q + \frac{1}{2}\gamma D A_b N_\gamma + \pi d L \sigma_v K_s tan\delta + \gamma H_t A_t N_q + \frac{1}{2}\gamma D A_t N_\gamma \quad [2]$$

Where, H_b (= 3 m), H_t (= 3 m (P1C), 1.86 m (P2C), 1.09 m (P3C) and 0.33 m (P4C)) , E, and L stand for the depth to bottom helix, depth to top helix, lower helix embedment, and total length of pile, respectively; σ_v is the overburden stress; K_s states the coefficient of lateral earth pressure in compression loading (see Perko (2009)); δ (=0.75 ϕ_{CV}) refers to the interface friction angle between soil and pile material; A_s, A_b, and A_t, indicates the surface area of the smooth, net area at the bottom helix, and net area at the top helix of the piles, respectively and N_q, N_γ are the dimensionless bearing capacity factors for the local shear condition and N_t refers to toe bearing capacity factor of the smooth pile (refer to CFEM 2006).

Fig. 11 plots the estimated Q_u from Eq. 1 & 2 with measured Q_u at 15% w/d (for P0C) and 5% w/D (for P1C-P4C). The coefficient of determination (R^2) of the estimated and measured ultimate capacity was 0.893, which indicates a relatively strong prediction. However, the theoretical equations from CFEM (2006) underestimated the capacity for piles P1C and P4C. Moreover, with increased helix spacing (from P2C to P4C), CFEM (2006) predicts a decrease in capacity. The possible cause for a higher measured value of Q_u for pile P1C might be the higher relative density of sand around the pile caused due to disturbances while installing this particular pile type. It is to note that, the pluviated sand on the model sand box showed signs of non-uniformity while deposition on the model box. However, the average relative density on the model box was within the estimated range. The measured Q_u was observed also higher for piles with larger spacing (i.e., in P4C), and it decreased gradually by lowering the spacing to 1.5 (in P2C). The reason for a higher capacity in P4C might be the accumulation of a larger column of soil

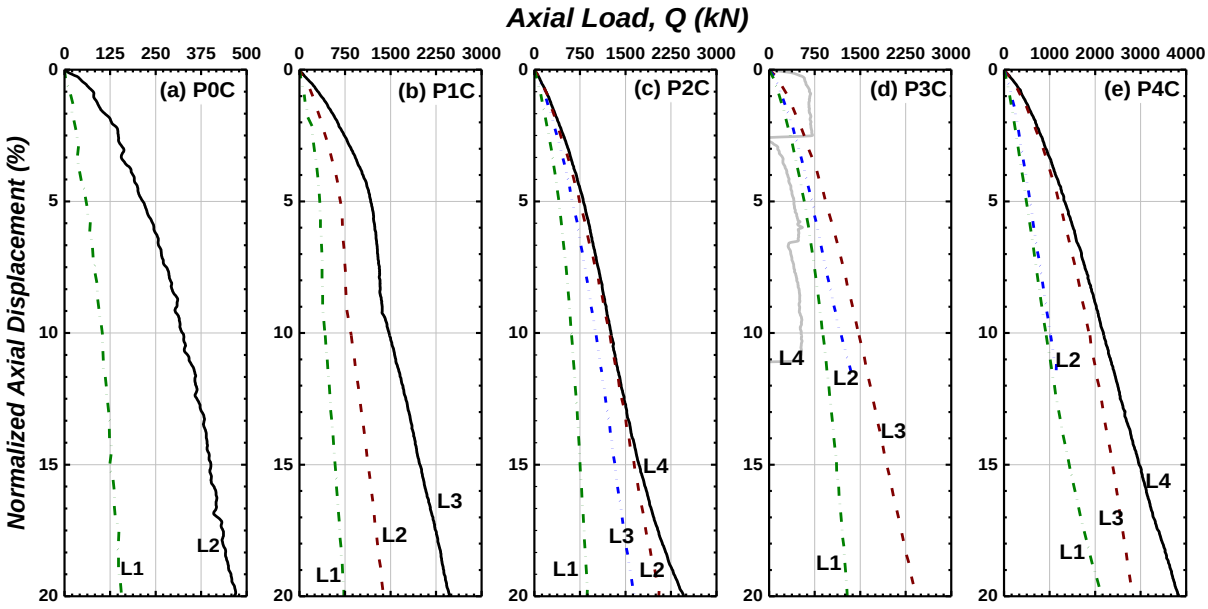

Figure 10. Axial Load (Q_u) vs. Normalized axial displacement (w/d for P0C and w/D for P1C-P4C) curves of the modeled piles. L1 to L4 are axial strain gauge stations labeled from the tip to the rear end of the piles.

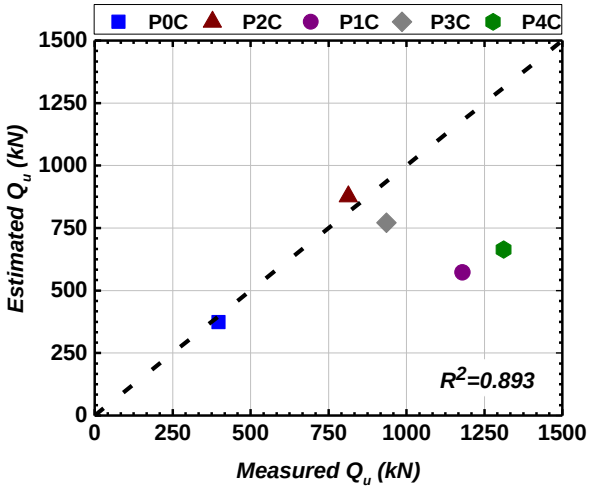

Figure 11. Estimated Q_u from CFEM (2006) vs. Measured Q_u at 15% w/d (for P0C) and at 5% w/D (for P1C-P4C).

within the inter helix space that generated larger resistances with the nearby soil out of the helices as typically observed in a cylindrical shear mode (CSM) condition.

4 CONCLUSIONS

An overview of the centrifuge testing for axially loaded helical piles is presented. The study aims to ascertain the behavior of smooth pile and helical piles and their interaction with the nearby soil. Firstly, a summary of the axial strain gauge installation, instrumentation, and calibration setup was shown. Then, the centrifuge test setup was elaborated. A calibration chart was developed for a portable traveling pluviator for preparing the sand bed within the model box at a definite relative density. Five model piles were installed at a 1 g model scale and later tested at 20 g acceleration in the sand at the GeoCERF facility. The compressive load-displacement responses for each pile were presented, noting the difference at each SG station along the pile length. It was observed that the capacity was significantly higher in helix piles compared to smooth piles. Finally, a comparison with the estimated ultimate capacity from CFEM (2006) to the measured Q_u from the centrifuge tests is shown. The estimated Q_u was comparable to the measured Q_u for piles P0C, P2C, and P3C. However, the test over predicted the capacity for pile type P1C and P4C. But, with increased inter helix spacing of the pile, measured Q_u increased, as in a cylindrical shear mode (CSM) criterion.

The results presented here are from an ongoing project of helical pile research in the sand at the University of Alberta. The tests were conducted recently and are therefore considered preliminary for the current stage. Hence, detailed results will be followed in future publications.

5 ACKNOWLEDGEMENTS

This project is funded by the Natural Sciences and Engineering Research Council of Canada (NSERC) and Reaction Piling Inc., Nisku, Alberta, Canada. The authors appreciate the assistance of Weidong Li, Yazhao Wang, Dmytro Pantov, and Jianlong Liu from the University of Alberta. The development of the Centrifuge (GeoCERF) facility was supported by the Canadian Foundation for Innovation.

6 REFERENCES

Al-Baghdadi, T.A., Brown, M.J. and Knappett, J.A. 2016. Development of an inflight centrifuge screw pile installation and loading system, In *3rd European*

Conference on Physical Modelling in Geotechnics. 239-244.

Arai, M.J., Fujii, M. and Watanabe, K. 2011. Thermal analysis of soil surrounding the screw piles using the infrared camera, In *The Twenty-first International Offshore and Polar Engineering Conference*. OnePetro.

AS 4678-2002 Earth retaining structures, Australian Standard

ASTM D 1143/D 1143M-20 Standard Test Methods for Deep Foundation Element Under Static Axial Compressive Load.

Bian, Y., Hutchinson, T.C., Wilson, D., Laefer, D. and Brandenberg, S. 2008. Experimental investigation of grouted helical piers for use in foundation rehabilitation, Journal *of Geotechnical and Geoenvironmental Engineering*, 134(9):1280-1289.

Bolton, M. D. 1979. A Guide to Soil Mechanics. Macmillan, London, 456p

Bolton, M.D. 1986. The strength and dilatancy of sands. *Geotechnique* 36(1):65–78.

Brown, M., Davidson, C., Brennan, A., Knappett, J., Cerfontaine, B., and Sharif, Y. 2019. Physical modeling of screw piles for offshore wind energy foundations, In *1st International Symposium on Screw Piles for Energy Applications*.

CFEM. 2006. Canadian Foundation Engineering Manual. 4th ed. Canadian Geotechnical Society, BiTech Publisher Ltd., Canada.

Choi, S.K., Lee, M.J., Choo, H., Tumay, M.T. and Lee, W., 2010. Preparation of a large size granular specimen using a rainer system with a porous plate. *Geotechnical Testing Journal*, *33*(1):45-54.

Clemence, S.P., Crouch, L.K., and Stephenson, R.W. 1994. Prediction of uplift capacity for helical anchors in sand, In *Proceedings of the 2nd Geotechnical Engineering Conference, Cairo, Egypt*, 1: 332-343.

Elsherbiny, Z.H. and El Naggar, M.H. 2013. Axial compressive capacity of helical piles from field tests and numerical study, *Canadian Geotechnical Journal*, *50*(12):1191-1203.

Ghaly, A., Hanna, A. and Hanna, M. 1991. Uplift Behavior of Screw Anchors in Sand. I: Dry Sand, *Journal of Geotechnical Engineering*, 117(5):773-793.

Islam, N., Li, W. and Deng, L. 2020. Geotechnical Centrifuge Modelling in Canada, *Canadian Geotechnique*, Canadian Geotech Society Quarterly Magazine, 5-7.

Levesque, C.L., Wheaton, D.E. and Valsangkar, A.J. 2003. Centrifuge Modeling of Helical Anchors in Sand, *Proceedings of the 12th Pan-American Conf. on Soil Mechanics and Foundation Engineering*, 2: 1859-1863.

Li, W., Deng, L. and Chalaturnyk, R. 2022. Centrifuge modeling of the behavior of helical piles in cohesive soils from installation and axial loading. *Soils and Foundations*, 62(3):101141.

Livneh, B. and El Naggar, M.H. 2008. Axial testing and numerical modeling of square shaft helical piles under compressive and tensile loading, *Canadian Geotechnical Journal*, 45(8):1142-1155.

Mitsch, M. P. and Clemence, S. P. 1985. The uplift capacity of helix anchors in sand, Uplift behavior of anchor foundations in soil. Proc, ASCE, New York, N.Y., 26-47.

Nabizadeh, F. and Choobbasti, A.J. 2017. Field study of capacity helical piles in sand and silty clay, *Transportation Infrastructure Geotech*, 4(1): 3-17.

Nagata, M. and Hirata, H. 2005. Study on uplift resistance of screwed pile. Nippon Steel Tech. Report,92: 73-78

Perko, H. A. 2009. Helical piles: a practical guide to design and installation. John Wiley & Sons.

Reese, L.C., and O'Neill, M.W. 1988. Drilled shafts. Construction procedures and design methods, Federal Highway Administration, Washington, DC Publication No. FHWA-HI-88-042.

Schiavon, J.A., Tsuha, C.D.H.C. and Esquivel, E.R. 2013. Application of two dimensional photoelastic analysis study of helical anchors, In *1st International Geotechnical Symposium on Helical Foundations,* 262-271.

Schiavon, J. A., Tsuha, C. D. H. C., and Thorel, L. 2016. Scale effect in centrifuge tests of helical anchors in sand, *International Journal of Physical Modeling in Geotechnics*, 16(4):185-196.

Sakr, M. 2009. Performance of helical piles in oil sand. *Can. Geotechnical Journal*, 46(9):1046-1061.

Sakr, M. 2011. Installation and performance characteristics of high capacity helical piles in cohesionless soils. *DFI Journal-The Journal of the Deep Foundations Institute*, 5(1): 39-57.

Spagnoli, G., Gavin, K., Brangan, C., and Bauer, S. 2015. In situ and laboratory tests in dense sand investigating the helix-to-shaft ratio of helical piles as a novel offshore foundation system, *Frontiers in Offshore Geotechnics*, 3: 643-648.

Tabaroei, A., Abrishami, S. and Hosseininia, E.S. 2017. Comparison between two different pluviation setups of sand specimens, *Journal of Materials in Civil Engineering*, *29*(10): 04017157.

Tsuha, C.D.H.C., Aoki, N., Rault, G., Thorel, L. and Garnier, J. 2007. Physical modelling of helical pile anchors, *International Journal of Physical Modelling in Geotechnics*, *7*(4): 01-12.

Tsuha, C.D.H.C., Aoki, N., Rault, G., Thorel, L. and Garnier, J., 2012. Evaluation of the efficiencies of helical anchor plates in sand by centrifuge model tests, *Canadian Geotechnical Journal*, 49(9):1102-1114.

Tsuha, C.D.H.C., Santos, T.D.C., Rault, G., Thorel, L. and Garnier, J., 2013. Influence of multiple helix configuration on the uplift capacity of helical anchors, In *Proceedings of the 18th International conference on soil mechanics and geotechnical engineering,* 2595.

Urabe, K., Tokimatsu, K., Suzuki, H. and Asaka, Y. 2015. Bearing capacity and pullout resistance of wing piles during cyclic vertical loading, In *Proceedings of the 6th International Conference on Earthquake Geotechnical Engineering*, 358-367.

Wang, D., Merifield, R.S. and Gaudin, C. 2013. Uplift behaviour of helical anchors in clay, *Canadian Geotechnical Journal*, *50*(6): 575-584.

Zhang, D. 1999. Predicting capacity of helical screw piles in Alberta soils, M.Sc. thesis, *University of Alberta*, Edmonton, Alberta.